# A Unified Prompt-Guided In-Context Inpainting Framework for Reference-based Image Manipulations

Chenjie Cao, Qiaole Dong, Yikai Wang, Yunuo Cai, Yanwei Fu

School of Data Science Fudan University {20110980001, yanweifu}@fudan.edu.cn

## **Abstract**

Recent advancements in Text-to-Image (T2I) generative models have yielded impressive results in generating high-fidelity images based on consistent text prompts. However, there is a growing interest in exploring the potential of these models for more diverse reference-based image manipulation tasks that require spatial understanding and visual context. Previous approaches have achieved this by incorporating additional control modules or fine-tuning the generative models specifically for each task until convergence. In this paper, we propose a different perspective. We conjecture that current large-scale T2I generative models already possess the capability to perform these tasks but are not fully activated within the standard generation process. To unlock these capabilities, we introduce a unified Prompt-Guided In-Context inpainting (PGIC) framework, which leverages largescale T2I models to re-formulate and solve reference-guided image manipulations. In the PGIC framework, the reference and masked target are stitched together as a new input for the generative models, enabling the filling of masked regions as producing final results. Furthermore, we demonstrate that the self-attention modules in T2I models are well-suited for establishing spatial correlations and efficiently addressing challenging reference-guided manipulations. These large T2I models can be effectively driven by task-specific prompts with minimal training cost or even with frozen backbones. We synthetically evaluate the effectiveness of the proposed PGIC framework across various tasks, including reference-guided image inpainting, faithful inpainting, outpainting, local super-resolution, and novel view synthesis. Our results show that PGIC achieves significantly better performance while requiring less computation compared to other fine-tuning based approaches. Models and codes are released in https://github.com/ewrfcas/PGIC\_inpainting.

# 1 Introduction

Recently, pioneering Text-to-Image (T2I) generative models [59; 63; 46; 40; 50; 48; 7; 65] have exhibited the ability to synthesize images of remarkable quality when furnished with suitable textual prompts. Their impressive generation capabilities have been extensively explored for personalization [15; 49; 38], controllable image-to-image generation [66; 39; 60; 5], and even 3D generation [42; 31; 33]. In contrast, this paper focuses on Reference-based image Manipulation (Ri-Mani) tasks that involve modifying target images using reference examples. Unlike pure generative tasks, Ri-Mani tasks demand the modified image parts to be consistent with the reference example based on certain rules. Critically, different from previous works of addressing each individual Ri-Mani task separately, *e.g.*, reference-guided inpainting [72; 70], and novel view synthesis [33], we present a unified framework to solve various Ri-Mani tasks by leveraging the capacity from large T2I models.



Figure 1: Illustration of reference-guided image manipulations (upper) addressed by PGIC. Benefiting from the large capacity of the T2I model, PGIC regards all these tasks as in-context inpainting with green-framed inputs and purple-framed generations. PGIC enjoys both computational efficiency and fast convergence, and can be generalized into high-fidelity image inpainting & oupainting (bottom).

The naïve solution for Ri-Mani tasks is to train additional adapters with zero-initialization [22; 66; 39] to the generative model. Unfortunately, such adapter-based fine-tuning strategies [66; 39] are limited to capturing fine-grained correlations, such as object orientations and locations between the reference and target images. But these factors are essential for Ri-Mani as evaluated in the pilot study of Tab. 1 for the reference-guided inpainting. Furthermore, as Ri-Mani tasks transition from text-guided to image-guided, some works replaced textual encoders with visual ones and fine-tuned the entire T2I model using hundreds of GPU hours [60; 33]. However, training these large T2I models with unfamiliar visual encoders is computationally intensive and difficult to converge with a limited batch size. Additionally, most visual encoders, such as image CLIP [44], tend to learn semantic features instead of fine-grained spatial ones, which are inadequate for addressing Ri-Mani tasks.

Our proposed solution aims to overcome the pitfalls of heavily re-training T2I generative models for Ri-Mani tasks. We start with the underlying insight that most generative T2I models come equipped with attention mechanisms that can extract spatial correlations from images and text. Thus, we ask whether these attention mechanisms have already established correlations between reference images and generative targets. To unlock this potential, we draw inspiration from [4] and re-formulate various Ri-Mani tasks into a unified in-context inpainting framework. Specifically, we stitch the reference condition and masked target into the same image, as shown in Fig. 1. Then, we use the pre-trained textual encoder and cross-attention modules to prompt-tune T2I models for specific tasks [53].

Formally, we propose the Prompt-Guided In-Context inpainting (PGIC) framework, which is a novel approach based on the off-the-shelf Latent Diffusion Model (LDM) [48]<sup>1</sup> that is fine-tuned with text-guided inpainting. PGIC is primarily designed to address various Ri-Mani tasks including reference-guided inpainting, reference-guided local Super-Resolution (SR), and novel view synthesis from a single image by placing reference conditions and masked targets on different sides of the same image. Furthermore, the task-specific prompt tuning [24; 53] is employed to control the generative tasks efficiently, which can be further generalized to achieve faithful inpainting and outpainting results without other guidance. Remarkably, our lightweight prompt tuning approach requires only 0.05M new parameters for each task while keeping all other weights from SD frozen. Even for the non-trivial task of reference-guided inpainting that usually requires sophisticated 3D geometrical warping and 2D inpainting [72; 70; 68], our PGIC framework can address it end-to-end with negligible new parameters. We further improve the training components gradually for more challenging scenarios such as local SR and novel view synthesis due to different input forms.

PGIC's novel in-context formulation results in faster convergence and efficient training, outperforming other baselines with the same training computation and parameters [66; 60; 33]. To the best of our

<sup>&</sup>lt;sup>1</sup>Stable Diffusion (SD) 2.0: https://github.com/Stability-AI/stablediffusion.

knowledge, we introduce task-specific prompt tuning for driving the generation of T2I models for the first time, making our PGIC framework a significant contribution to the field.

In summary, our contributions could be highlighted as follows: 1) Proposing a novel in-context inpainting-based formulation that unlocks the capability of large T2I models for Ri-Mani tasks. 2) Introducing task-specific prompt tuning to efficiently control the generation of T2I models with both parameter and computational efficiencies. 3) Demonstrating the substantial performance of our newly proposed PGIC in various generative tasks, including inpainting, outpainting, reference-guided inpainting, local SR, and novel view synthesis.

#### 2 Related Work

Personalization and Controllability of T2I Models. Recent achievements on T2I have produced impressive visual generations, which could be further extended into local editing [2; 18; 10]. However, these T2I models could only be controlled by natural languages. As "an image is worth hundreds of words", T2I models based on natural texts fail to produce images with specific textures, locations, identities, and appearances [15]. Textual inversion [15; 38] and fine-tuning techniques [49] are proposed for personalized T2I. Meanwhile, many works pay attention to image-guided generations [57; 28; 37]. ControlNet [66] and T2I-Adapter [39] learn trainable adapters [21] to inject visual clues to pre-trained T2I models without losing generalization and diversity. But these moderate methods only work for simple style transfers. More spatially complex tasks, such as reference-guided inpainting, are difficult to be addressed by ControlNet as verified in Sec. 4. In contrast, T2I-based exemplar-editing and novel view synthesis have to be fine-tuned on large-scale datasets with strong data augmentation [60] and large batch size [33]. Compared with these aforementioned manners, the proposed PGIC enjoys both spatial modeling capability and computational efficiency.

**Prompt Tuning** [26; 35; 34] indicates fine-tuning token embeddings for transformers with other parameters frozen to preserve the capacity. Prompt tuning is first explored in Natural Language Processing (NLP) for adaptively learning suitable prompt features for language models rather than manually selecting them for different downstream tasks [32]. Moreover, prompt tuning has been further investigated in vision-language models [44; 61; 16] and discriminative vision models [24; 3; 30]. Visual prompt tuning in [53] prepends trainable tokens before the visual sequence for transferred generations. Though both PGIC and [53] aim to tackle image synthesis, our prompt tuning is used for driving text encoders of T2I models rather than visual ones. Thus PGIC enjoys more intuitive prompt initialization from task-related textual descriptions (Sec. 4.4). Besides, we should clarify that prompt tuning is different from textual inversion [15]. Prompt tuning is used to address specific downstream tasks, while textual inversion tends to present personalized image subsets.

Image Inpainting and In-Context Learning. Image inpainting is a long-standing vision task, which aims to fill missing image regions with perceptually pleasant and visually vivid results. Both traditional methods [6; 11; 17] and learning-based ones [64; 69; 27; 55; 13] achieved great progress in image inpainting. Furthermore, reference-guided inpainting requires recovering a target image with one or several reference views [41], which is useful to repair old buildings or remove occlusions in popular attractions. But reference-guided inpainting usually suffers from a sophisticated pipeline [72; 70; 68], which includes depth estimation, pose estimation, homography warping, and single view inpainting. Note that for large holes, the geometric pose is not reliable; and the pipeline will be largely degraded. Thus an end-to-end reference-guided inpainting pipeline is meaningful. On the other hand, Bar *et al.* [4] propose to formulate inpainting as a pretext task and further learn image-to-image translations through the in-context learning. Formally, given an image-to-image example, then the unseen transfer task could be addressed as grid-based inpainting. Some follow-ups improve the training and data formulation [58; 67]. To the best of our knowledge, we are the first ones to leverage this setting to tackle difficult reference-guided tasks with T2I models.

## 3 Prompt-Guided In-Context Inpainting

**Overview.** In this section, we first introduce the overall framework of the proposed PGIC and the critical task-specific prompt tuning in Sec. 3.1. Then, we analyze and define three types of representative Ri-Mani tasks addressed by PGIC (Sec. 3.2), and further discuss the specific data and model adaptations adopted by PGIC for different types of tasks (Sec. 3.3).

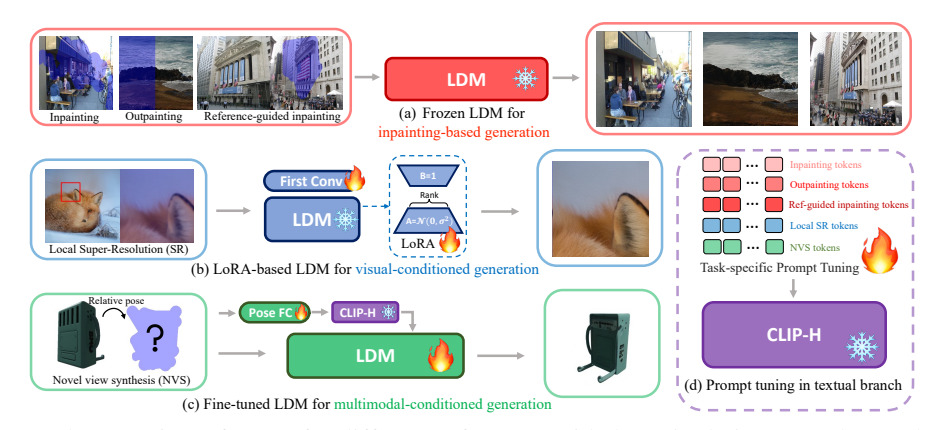


Figure 2: The overview of PGIC for different reference-guided manipulations. (a),(b),(c) show the visual branches for three different groups of Ri-Mani tasks. (d) shows the textual branch with prompt tuning. We omit the cross-attention between CLIP-H and LDM for simplicity.

#### 3.1 Framework of PGIC

The framework of PGIC is illustrated in Fig. 2, which is based on the inpainting pre-trained LDM [48]. Essentially, we re-formulate Ri-Mani tasks as the image inpainting problem. As all kinds of reference can be formatted as different forms of images, we define the reference image as a generic  $\mathbf{I}_{ref} \in \mathbb{R}^{H \times W}$ . Different tasks induce different forms of  $\mathbf{I}_{ref}$ . The standard approach of incorporating reference images into the generation process includes concatenation on the channel dimension of input images or adopting an extra image encoder for the network [66; 39; 60; 33]. However, both strategies require additional training to rebuild the correlation between the reference and target for the generative model, which is against our motivation for a unified framework unlocking the capability of large T2I models.

Thanks to the convolution-based U-net architecture in LDM, we can extend the input image in the spatial dimensions without extra modification. Our input  $\mathbf{I}'$  is the concatenation of  $\mathbf{I}_{ref}$  and the masked target  $\hat{\mathbf{I}}_{tar}$ , forming as  $\mathbf{I}' = [\mathbf{I}_{ref}; \hat{\mathbf{I}}_{tar}] \in \mathbb{R}^{H \times 2W}$ . For simplicity, we take the reference image on the left side, while the target one is placed on the right side as in Fig. 1. Masked targets could be generated successfully along with the PGIC filling the hole in the target side. The inpainting formulation fully exploits the in-context capability of pre-trained self-attention in LDM to address reference-guided tasks. However, text-guided inpainting requires image-dependent text prompts to guide the diffusion model to generate consistent images. It is non-trivial to define all reference-guided tasks with natural languages. On the other hand, it is beneficial to have an image-independent prompt to guide the diffusion model to perform specific tasks. To this end, we propose to use prompt tuning to learn task-specific prompts for each reference-guided task.

Task-Specific Prompt Tuning is adopted in all tasks as the textual branch of Fig. 2(d). Specifically, we prepare a set of trainable text embeddings for each generative task. Though there are only a few trainable parameters (0.05 M to 0.07 M), we astonishingly find that prompt tuning is sufficient to drive the complex generative task such as reference-guided inpainting, even though the LDM backbone is completely frozen. The trainable prompt embeddings p are initialized as the averaged embedding of the natural task description. The optimization target can be defined as

$$p_* = \arg\min_{p} \mathbb{E}_{x,\epsilon \sim \mathcal{N}(0,\mathcal{I}),t} \left[ \|\varepsilon - \varepsilon_{\theta} \left( [z_t; \hat{z}_0; \mathbf{M}], c_{\phi}(p), t \right) \|^2 \right], \tag{1}$$

where  $\varepsilon_{\theta}(\cdot)$  is the estimated noise by LDM;  $c_{\phi}(\cdot)$  means the frozen CLIP-H;  $z_t$  is a noisy latent feature of input  $z_0$  in step t;  $\hat{z}_0 = z_0 \odot (1-\mathbf{M})$  are masked latent features that are concatenated to  $z_t$  with mask  $\mathbf{M}$ . Tasks-specific prompt tuning enjoys not only training efficiency but also lightweight saving [26]. For example, we could address many different applications with the same PGIC, while only 0.01% additional weights of  $p_*$  are required to be changed for each task.

As PGIC only learns a task-specific prompt for each Ri-Mani task, it is natural to combine this strategy with more fine-tuning strategies to further improve the applicability of PGIC. Intuitively, when a Ri-Mani task is similar to the original inpainting task pre-trained by LDM, it is expected that a task-specific prompt is enough to guide the generation process. When a task is far from the

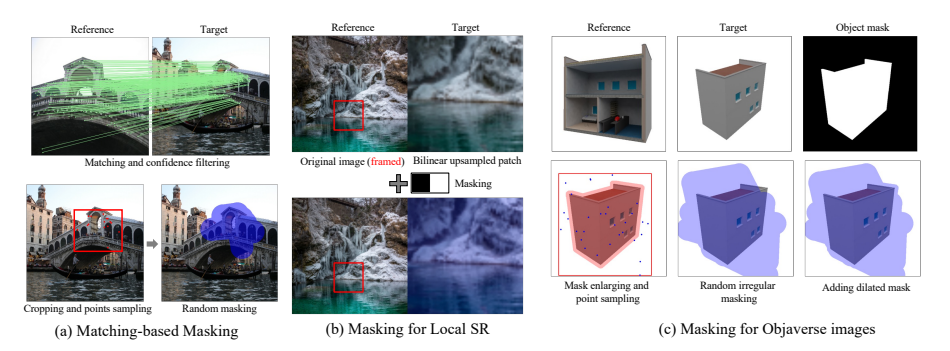


Figure 3: The illustration of (a) matching-based masking for reference-guided inpainting, (b) masking for local SR, and (c) masking strategy used for novel view synthesis on Objaverse [12].

inpainting task, it may be beneficial to fine-tune the diffusion model for better adaptation. Note that even the simplest Ri-Mani task can not be trivially regarded as the vanilla inpainting task. Because we require to retain a certain rule-based consistency between the generated image and the reference one rather than simply generating images with seamless appearances.

#### 3.2 Different Task Formulations for PGIC

To better adapt PGIC to different Ri-Mani tasks, we analyze their similarities and difficulties compared with the vanilla image inpainting and further categorize them into three groups: *inpainting-based*, *visual-conditioned*, and *multimodal-conditioned* generations.

**Inpainting-based Generation** includes image inpainting, outpainting<sup>2</sup>, and reference-guided inpainting, to name a few. These tasks could be still regarded as image inpainting essentially, so it is unnecessary to adjust the input formulation for them. Unlike the 'one-for-one' text prompts used in LDM inpainting, there are no common manual prompts that can be applied to all images with the same aim. Without specific text descriptions, inpainting and outpainting suffer from uncontrollable hallucinations. Instead, trainable prompts are incorporated to drive the image inpainting for different masking styles with faithful and high-fidelity inpainted results as well as reference-guided inpainting.

**Visual-Conditioned Generation** indicates image-to-image tasks where all conditions are based on visuals but can not be formulated as image inpainting directly. We take the local SR as an example in this paper. Local SR needs to magnify a specific patch of the original image into high resolution. So the original image could be seen as the reference condition for global information, while we apply the upsampled local patch framed in the reference as the target base.

**Multimodal-Conditioned Generation** requires additional meta information beyond the images, such as camera poses or class labels. In this paper, we take the challenging novel view synthesis from a single image as an example. Actually, without the geometric consistency from multi-view images, the single-view-based novel view synthesis is an ill-posed and intractable task. But the encouraging successes from some text-to-3D works [42; 31] demonstrate that the large capacity from pre-trained T2I models could facilitate geometric understanding.

#### 3.3 Data and Model Adaptation for PGIC

For three different groups of Ri-Mani tasks mentioned in Sec. 3.2. We propose different variants of data process and model design in Fig. 3 and Fig. 2(a)(b)(c) respectively.

**Inpainting-based Generation.** For the reference-guided inpainting, we find that the widely used irregular mask [13; 72; 70] fails to reliably evaluate the capability of spatial transformation and structural preserving. Therefore, we propose the matching-based masking as shown in Fig. 3(a). Specifically, we use a feature matching model [56] to detect matching pairs between reference and target images filtered by a high confidence score. Then we crop a sub-space in the matched region and randomly sample some matching pairs as vertices to be painted across for the final masks. The matching-based mask not only improves the reliability during the evaluation but also facilitates the performance in the training phase. For the model design, *frozen LDM* is utilized to address

<sup>&</sup>lt;sup>2</sup>For simplicity, here we also regard inpainting and outpainting as Ri-Mani tasks (masking-based generation).

inpainting-based tasks as in Fig. 2(a), while only prompt tuning is demanded. We should clarify that such an efficient setting enjoys prominent improvements compared with other baselines especially for the reference-guided inpainting as in Tab. 1.

**Visual-Conditioned Generation.** For the local SR, we directly attach the red frame to the reference image as in Fig. 3(b), while the prompt tuning based large T2I models are sufficient to understand this in-context annotation. The upsampled target patch is resized by bilinear; we still provide a mask channel to prompt PGIC that the target side should be further refined. We empirically find such a low-resolution base largely improves the performance. Moreover, the Low-Rank Adaptation (LoRA) [22] based fine-tuning is adopted to tackle the visual-conditioned generation as in Fig. 2(b). Though all input conditions are based on visuals, lightweight fine-tuning is critical to fill the gap to vanilla inpainting. We find that the efficient LoRA is sufficient to achieve competitive results compared with the whole model fine-tuning. Furthermore, since input features are different from ones used in inpainting, *i.e.*, the unseen masked regions are replaced with known low-resolution patches, fine-tuning the first convolution of LDM enjoys a good improvement with negligible cost (Tab. 10).

Multimodal-Conditioned Generation. For the novel view synthesis, we first dilate the object mask and randomly sample points in the enlarged mask bounding box to paint the irregular mask. Then, we unite the dilated object mask to completely cover target images as in Fig. 3(c). We find that local masking is still very important for fast convergence and stable fine-tuning as empirically verified in experiments. For the relative pose parameters, we follow [33] to convert the pose into a spherical coordinate system with polar angle, azimuth angle, and radius distance. More details are discussed in the supplementary. To adapt multi-modal inputs, we fine-tune the whole LDM as shown in Fig. 2(c). An additional MLP layer is used to project pose parameters into a text embedding, which is further encoded by the CLIP model. Interestingly, regarding the projected pose feature as one textual embedding before the CLIP is sufficient to guide the synthesis of new viewpoints. Though learning non-visual features is relatively hard for PGIC, the proposed inpainting-based formulation still outperforms the competitor [33] with much fewer computational resources as verified in Sec. 4.3.

# 4 Experiments

**Datasets.** The inpainting and outpainting are evaluated on Places2 [71] and Flickr-Scenery [9] dataset respectively. For the reference-guided inpainting, we use image pairs from MegaDepth [29], which includes many multi-view famous scenes collected from the Internet. To trade-off between the image correlation and the inpainting difficulty, we empirically retain image pairs with 40% to 70% cooccurrence. And the validation also includes some manual masks from ETH3D scenes [51] to verify the generalization. For local SR, we evaluate our method on the mixed DIV2K and Flickr2K [1] from  $64 \times 64$  to  $256 \times 256$ . For the novel view synthesis from a single image, we use Objaverse [12] rendered by [33] including 800k various scenes with object masks. More details are in the supplementary.

**Implementation.** Our PGIC is based on the inpainting fine-tuned SD [48] with 0.8 billion parameters. Prompts with a length of 50 are used for most tasks of PGIC, while novel view synthesis uses a length of 73. All tasks are optimized with AdamW with a weight decay of 0.01. For inpainting-based tasks, the learning rate for prompt tuning is 3e-5, while we raise it to 1e-4 for other tasks. Further, the learning rate for the SD fine-tuning is 1e-5. For the reference-guided inpainting, 75% masks are randomly generated, and 25% of them are matching-based masks. All training is done with two 48G A6000 GPUs. More training details are listed in the supplementary.

# 4.1 Results of Inpainting-based Generation

Reference-Guided Inpainting. We thoroughly compared existing image reference-based variants of LDM in Tab. 1 and Fig. 4. Note that ControlNet [66] fails to learn the correct spatial correlation between reference images and masked targets, even enhanced with trainable cross-attention learned between reference and target features. Furthermore, we try to warp ground-truth latent features with image matching [56] as the reference guidance for ControlNet, but the improvement is not prominent. Perceiver [23] and Paint-by-Example [60] align and learn images features from ImageCLIP [44]. Since image features from CLIP contain high-level semantics, they could not deal with the finegrained reference-guided inpainting as shown in Fig. 4(e)(f). For the reference-guided inpainting, TransFill [72] suffers from blur and color difference as in Fig. 4(g) Our PGIC enjoys substantial advantages in both qualitative and quantitative comparisons with negligible trainable weights.

Table 1: Quantitative results for reference-guided inpainting on MegaDepth [29] test set based on matching and manual masks. 'ExParams' means the scale of extra trainable parameters. Note \* means that the uncorrupted ground truth is visible for the matching as a competitor.

Methods	PSNR↑	SSIM↑	FID↓	LPIPS↓	ExParams
SD (inpainting) [48]	19.841	0.819	30.260	0.1349	+0
ControlNet [66]	19.072	0.744	33.664	0.1816	+364.24M
ControlNet+CrossAttn	19.027	0.743	34.170	0.1805	+463.41M
ControlNet+Matching* [56]	20.592	0.763	29.556	0.1565	+364.29M
Perceiver+ImageCLIP [23]	19.338	0.745	32.911	0.1751	+52.01M
Paint-by-Example [60]	18.351	0.797	34.711	0.1604	+865.90M
PGIC	20.926	0.836	18.680	0.0961	+0.05M

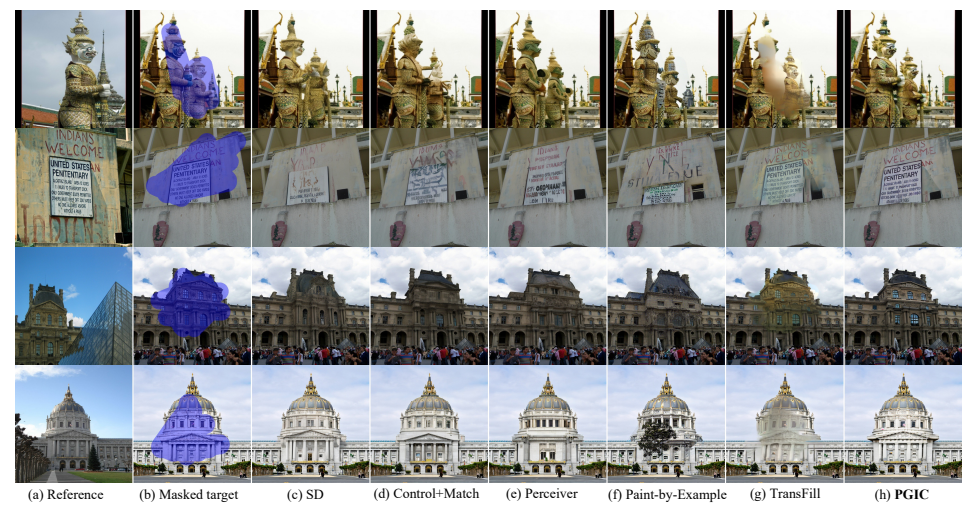


Figure 4: Qualitative reference-guided inpainting results on MegaDepth, which are compared among (c) SD [48], (d) ControlNet [66]+Matching [56], (e) Perceiver [23] with ImageCLIP [44], (f) Paintby-Example [60], (g) TransFill [72], and (I) our PGIC. Please zoom in for more details.

**Image Inpainting & Outpainting.** To show the effectiveness of the task-specific prompt tuning, we further try the prompt tuning on inpainting and outpainting in Tab. 2. Prompt-tuned PGICs achieve substantially better results compared with vanilla inpainting-based SD. Note that it is quite difficult to use one natural word or sentence to prompt inpainting and outpainting, such as "background" verified in Tab. 2. We also find that PGIC enjoys fewer hallucinatory artifacts as shown in the supplementary.

## 4.2 Results of Local Super-Resolution

We evaluate the exploratory local SR in Tab. 10 and Fig. 5. Though the pure prompt tuning is not powerful enough, PGIC based on LoRA [22] of low-rank 64 can be well generalized into local SR with only 20M trainable weights. Moreover, training the first convolution in SD can further narrow the input gap. Moreover, PGIC enjoys competitive or superior qualitative results compared with SR-specific LIIF [8] and reference-based MASA-SR [36]. PGIC benefits a lot from the global understanding of the reference. For example, PGIC reconstructs better details for the railing in Fig. 5.

Table 2: Quantitative results for inpainting on Places2 [71] and outpainting on Flickr-Scenery [9].

Mathada	Duament	Inpainting				Outpainting			
Methods	Prompt	PSNR↑	SSIM↑	FID↓	LPIPS↓	PSNR↑	SSIM↑	FID↓	LPIPS↓
Co-Mod [69]	/	21.091	0.843	30.041	0.1664	_	_	_	_
MAT [27]	/	20.680	0.838	32.439	0.1650	_	_	_	_
SD (inpainting)	None	20.353	0.839	29.632	0.1603	14.476	0.693	53.523	0.3475
SD (inpainting)	"background"	20.591	0.844	29.313	0.1564	14.601	0.696	46.582	0.3429
PGIC (prompt tuning)	Trainable (len50)	21.982	0.869	24.401	0.1295	15.989	0.731	29.056	0.3131

Toble 2. Desults for least CD	on mixed DIV2K/Flickr2K testset.	Einel adopted settings one in held
Table 5 Results for local 5R	ON MIXED IN V/K/PHCKT/K JESISEL	rinai adonied seifings are in noid

Methods	Rank	PSNR↑	SSIM↑	FID↓	LPIPS↓	ExParams
LDM (SR)	1	24.379	0.790	46.716	0.2005	/
PGIC (prompt tuning) PGIC (fine-tuning) PGIC (LoRA) PGIC (LoRA)	/	23.668	0.775	57.976	0.2411	+0.05M
	/	<b>25.640</b>	<b>0.799</b>	38.832	0.1519	+865.9M
	r=64	25.500	0.795	38.619	0.1557	+20.52M
	r=128	25.445	0.794	<b>38.315</b>	<b>0.1530</b>	+40.99M
+ First conv trainable - Reference image	r=64	25.589	0.798	38.477	0.1556	+0.003M
	r=64	25.209	0.789	39.108	0.1580	/

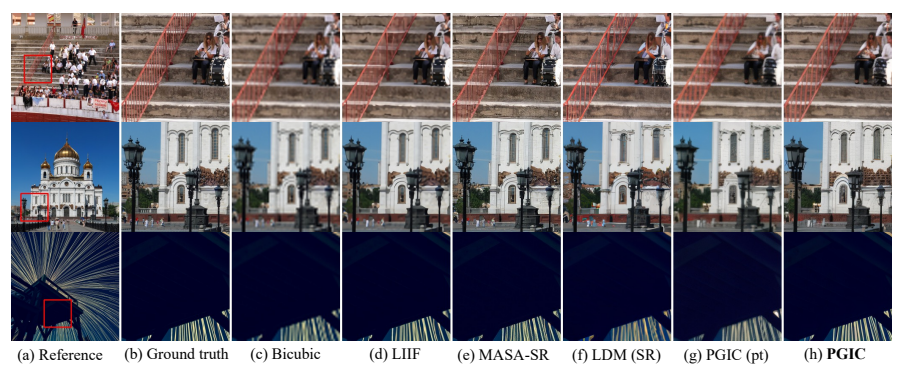


Figure 5: Qualitative local SR results. (c) bicubic, (d) LIIF [8], (e) MASA-SR [36], (f) LDM (SR) [48], (g) PGIC (prompt tuning), and (h) PGIC based on LoRA on DIV2K and Flickr2K.

#### 4.3 Results of Novel View Synthesis

The novel view synthesis from a single view is a very challenging issue with geometric ambiguity. We explore the feasibility to learn this task with limited resources as in Tab. 4 and Fig. 6. The CLIP score [44] is compared to evaluate the similarity between the generation and the target. Prompt tuning and LoRA-based fine-tuning are insufficient to achieve high-fidelity results as in Tab. 4. Fine-tuning the whole LDM enjoys substantial improvements. But all variants of PGIC outperform the state-of-the-art competitor Zero123 [33] with the same training setting (batch size 48 with 2 A6000 GPUs) in Tab. 4 because the latter needs much larger batch size (1536) for a stable training. Thus our in-context inpainting-based PGIC enjoys a good balance between training efficiency and performance. Moreover, we evaluate the effectiveness of Classifier-Free Guidance (CFG) [20] during the training phase, which enjoys better pose guidance with a CFG coefficient 2.5 for the inference. Besides, encoding additional pose features (Pose encoding in Tab. 4) rather than the pose projected textual embedding mentioned in Sec. 3.3 does not achieve more improvement. It indicates that one textual feature from CLIP is sufficient to guide directions and poses of the object generation.

**Adaptive Masking.** One may ask that the masking strategy used in Fig. 3(c) suffers from some shape leakages, which lead to unreliable metrics in Tab. 4. We should clarify that PGIC can perform well only with the reference mask, which is easy to get by the salient object detection [43]. Specifically, we dilate the reference mask as Fig. 3(c). Then few DDIM steps [54] are used to generate a rough synthesis in the target view. After that, we detect the foreground mask based on the rough synthesis by [43] and further dilate this mask for the second synthesis with full DDIM steps. The adaptive masking can be well generalized to the novel view synthesis as verified in Tab. 4 and Fig. 7. Besides,



Figure 6: Novel view synthesis on Objaverse [12] from a single reference image.

Table 4: Results for novel view synthesis with a single image on Objaverse [12]. Zero123\* is re-trained with the same training setting as our method. The final adopted settings are in bold.

Methods	PSNR↑	SSIM↑	LPIPS↓	CLIP↑
Zero123* [33] PGIC (prompt tuning) PGIC (LoRA) PGIC (fine-tuning)	13.138	0.794	0.3553	0.6630
	15.164	0.846	0.2652	0.6944
	18.286	0.883	0.1644	0.7367
	19.215	0.891	0.1394	0.7635
+ CFG training (0.15)	<b>19.555</b>	<b>0.892</b>	<b>0.1355</b>	0.7630
+ Pose encoding	19.321	0.891	0.1401	0.7640
+ Adaptive mask	18.963	0.886	0.1553	<b>0.7657</b>



Figure 7: Long sequence synthesis from a single image (upper) with adaptive masking (bottom). The leftmost image and mask are the input while others are generated.

we think that providing target masks according to the distance and direction priors manually is also convincing to address the challenging single-view-based novel view synthesis.

Table 5: Ablation studies for the prompt length of reference-guided inpainting. 'Shallow' means only prompt tuning to text embedding, while 'Deep' indicates tuning additional embedding features to different cross-attention layers (16 layers) in the SD.

Prompt Type	Length	PSNR↑	SSIM↑	LPIPS↓	ExParams
Shallow Shallow Shallow	25 50 75	20.352 <b>20.489</b> 20.383	0.827 <b>0.829</b> <b>0.829</b>	0.1038 <b>0.1029</b> 0.1038	+0.025M +0.05M +0.075M
Deep	25 (425)	20.146	0.825	0.1059	+0.425M

Table 6: Ablation studies of reference-guided inpainting on MegaDepth. Left: effects of matching-based masks and inference noise  $\eta$ . Right: effects of different prompt initialization.

Configuration	PSNR↑	SSIM↑	LPIPS↓	Prompt init	PSNR↑	SSIM↑	LPIPS↓
baseline	20.489	0.829	0.1029	Random	20.810	0.832	0.0998
+ Match mask	20.574	0.830	0.1010	Token-wise	20.852	0.833	0.1002
+ η=1.0	<b>20.926</b>	<b>0.836</b>	<b>0.0961</b>	Token-avgs	<b>20.926</b>	<b>0.836</b>	<b>0.0961</b>

#### 4.4 Ablation Studies

**Prompt Length and Depth.** The length and depth used in the task-specific prompt tuning are explored in the ablation in Tab. 5. Different from [24], we find the PGIC is relatively robust in the length selection. Thus we select 50 in most cases, while we increase it to 73 to tackle novel vie synthesis. Moreover, we find that the deep prompt with much more trainable prompts for different cross-attention layers does not perform well, which may suffer from a little overfitting.

**Matching-based Masks and Noise Coefficient.** On the left of Tab. 6, we find that the matching-based mask enjoys substantial improvement in the reference-guided inpainting. Besides, we find that setting the noise coefficient  $\eta=1$  achieves consistent improvements in our PGIC even sampled as the DDIM [54]. So all LDMs are worked under  $\eta=1$  without special illustrations.

**Prompt Initialization.** We tried three initialization ways for the prompt tuning on the right of Tab. 6. The random initialization performs worst. Both 'token-wise' and 'token-avgs' leverage text embeddings from a task-specific descriptive sentence that is detailed in the supplementary. 'Token-wise' means repeating descriptive sentences until the prompt length, while each token is initialized for one prompt token. 'Token-avgs' indicates that all prompt tokens are initialized with the average of the descriptive sentence. Meaningful initialization is useful for task-specific prompt tuning.

#### 5 Conclusion

In this paper, we propose PGIC, which unifies Ri-Mani tasks as the in-context inpainting and addresses them end-to-end. Benefiting from the prompt tuning and the well-learned attention modules in large T2I models, PGIC can address the spatially sophisticated reference-guided inpainting efficiently. Moreover, the proposed PGIC can be successfully transferred to address other intractable Ri-Mani tasks with adaptive data and model designs, such as local SR and novel view synthesis with a single view. Comprehensive experiments on multiple generative tasks show the effectiveness of PGIC.

#### References

- [1] Eirikur Agustsson and Radu Timofte. Ntire 2017 challenge on single image super-resolution: Dataset and study. In *Proceedings of the IEEE conference on computer vision and pattern recognition workshops*, pages 126–135, 2017.
- [2] Omri Avrahami, Dani Lischinski, and Ohad Fried. Blended diffusion for text-driven editing of natural images. In *Proceedings of the IEEE/CVF Conference on Computer Vision and Pattern Recognition*, pages 18208–18218, 2022.
- [3] Hyojin Bahng, Ali Jahanian, Swami Sankaranarayanan, and Phillip Isola. Visual prompting: Modifying pixel space to adapt pre-trained models. *arXiv preprint arXiv:2203.17274*, 2022.
- [4] Amir Bar, Yossi Gandelsman, Trevor Darrell, Amir Globerson, and Alexei Efros. Visual prompting via image inpainting. Advances in Neural Information Processing Systems, 35:25005– 25017, 2022.
- [5] Omer Bar-Tal, Lior Yariv, Yaron Lipman, and Tali Dekel. Multidiffusion: Fusing diffusion paths for controlled image generation. *arXiv preprint arXiv:2302.08113*, 2, 2023.
- [6] Marcelo Bertalmio, Guillermo Sapiro, Vincent Caselles, and Coloma Ballester. Image inpainting. In *Proceedings of the 27th annual conference on Computer graphics and interactive techniques*, pages 417–424, 2000.
- [7] Huiwen Chang, Han Zhang, Jarred Barber, AJ Maschinot, Jose Lezama, Lu Jiang, Ming-Hsuan Yang, Kevin Murphy, William T Freeman, Michael Rubinstein, et al. Muse: Text-to-image generation via masked generative transformers. *arXiv preprint arXiv:2301.00704*, 2023.
- [8] Yinbo Chen, Sifei Liu, and Xiaolong Wang. Learning continuous image representation with local implicit image function. In *Proceedings of the IEEE/CVF conference on computer vision and pattern recognition*, pages 8628–8638, 2021.
- [9] Yen-Chi Cheng, Chieh Hubert Lin, Hsin-Ying Lee, Jian Ren, Sergey Tulyakov, and Ming-Hsuan Yang. Inout: diverse image outpainting via gan inversion. In *Proceedings of the IEEE/CVF Conference on Computer Vision and Pattern Recognition*, pages 11431–11440, 2022.
- [10] Guillaume Couairon, Jakob Verbeek, Holger Schwenk, and Matthieu Cord. Diffedit: Diffusion-based semantic image editing with mask guidance. *arXiv preprint arXiv:2210.11427*, 2022.
- [11] Antonio Criminisi, Patrick Perez, and Kentaro Toyama. Object removal by exemplar-based inpainting. In 2003 IEEE Computer Society Conference on Computer Vision and Pattern Recognition, 2003. Proceedings., volume 2, pages II–II. IEEE, 2003.
- [12] Matt Deitke, Dustin Schwenk, Jordi Salvador, Luca Weihs, Oscar Michel, Eli VanderBilt, Ludwig Schmidt, Kiana Ehsani, Aniruddha Kembhavi, and Ali Farhadi. Objaverse: A universe of annotated 3d objects. *arXiv preprint arXiv:2212.08051*, 2022.
- [13] Qiaole Dong, Chenjie Cao, and Yanwei Fu. Incremental transformer structure enhanced image inpainting with masking positional encoding. In *Proceedings of the IEEE/CVF Conference on Computer Vision and Pattern Recognition*, pages 11358–11368, 2022.
- [14] Patrick Esser, Robin Rombach, and Bjorn Ommer. Taming transformers for high-resolution image synthesis. In *Proceedings of the IEEE/CVF conference on computer vision and pattern recognition*, pages 12873–12883, 2021.

- [15] Rinon Gal, Yuval Alaluf, Yuval Atzmon, Or Patashnik, Amit H Bermano, Gal Chechik, and Daniel Cohen-Or. An image is worth one word: Personalizing text-to-image generation using textual inversion. *arXiv* preprint arXiv:2208.01618, 2022.
- [16] Chunjiang Ge, Rui Huang, Mixue Xie, Zihang Lai, Shiji Song, Shuang Li, and Gao Huang. Domain adaptation via prompt learning. arXiv preprint arXiv:2202.06687, 2022.
- [17] James Hays and Alexei A Efros. Scene completion using millions of photographs. *ACM Transactions on Graphics (ToG)*, 26(3):4–es, 2007.
- [18] Amir Hertz, Ron Mokady, Jay Tenenbaum, Kfir Aberman, Yael Pritch, and Daniel Cohen-Or. Prompt-to-prompt image editing with cross attention control. *arXiv preprint arXiv:2208.01626*, 2022.
- [19] Jonathan Ho, Ajay Jain, and Pieter Abbeel. Denoising diffusion probabilistic models. *Advances in Neural Information Processing Systems*, 33:6840–6851, 2020.
- [20] Jonathan Ho and Tim Salimans. Classifier-free diffusion guidance. arXiv preprint arXiv:2207.12598, 2022.
- [21] Neil Houlsby, Andrei Giurgiu, Stanislaw Jastrzebski, Bruna Morrone, Quentin De Laroussilhe, Andrea Gesmundo, Mona Attariyan, and Sylvain Gelly. Parameter-efficient transfer learning for nlp. In *International Conference on Machine Learning*, pages 2790–2799. PMLR, 2019.
- [22] Edward J Hu, Yelong Shen, Phillip Wallis, Zeyuan Allen-Zhu, Yuanzhi Li, Shean Wang, Lu Wang, and Weizhu Chen. Lora: Low-rank adaptation of large language models. *arXiv* preprint arXiv:2106.09685, 2021.
- [23] Andrew Jaegle, Felix Gimeno, Andy Brock, Oriol Vinyals, Andrew Zisserman, and Joao Carreira. Perceiver: General perception with iterative attention. In *International conference on machine learning*, pages 4651–4664. PMLR, 2021.
- [24] Menglin Jia, Luming Tang, Bor-Chun Chen, Claire Cardie, Serge Belongie, Bharath Hariharan, and Ser-Nam Lim. Visual prompt tuning. In *Computer Vision–ECCV 2022: 17th European Conference, Tel Aviv, Israel, October 23–27, 2022, Proceedings, Part XXXIII*, pages 709–727. Springer, 2022.
- [25] Justin Johnson, Alexandre Alahi, and Li Fei-Fei. Perceptual losses for real-time style transfer and super-resolution. In Computer Vision–ECCV 2016: 14th European Conference, Amsterdam, The Netherlands, October 11-14, 2016, Proceedings, Part II 14, pages 694–711. Springer, 2016.
- [26] Brian Lester, Rami Al-Rfou, and Noah Constant. The power of scale for parameter-efficient prompt tuning. *arXiv preprint arXiv:2104.08691*, 2021.
- [27] Wenbo Li, Zhe Lin, Kun Zhou, Lu Qi, Yi Wang, and Jiaya Jia. Mat: Mask-aware transformer for large hole image inpainting. In *Proceedings of the IEEE/CVF conference on computer vision and pattern recognition*, pages 10758–10768, 2022.
- [28] Yuheng Li, Haotian Liu, Qingyang Wu, Fangzhou Mu, Jianwei Yang, Jianfeng Gao, Chunyuan Li, and Yong Jae Lee. Gligen: Open-set grounded text-to-image generation. *arXiv* preprint *arXiv*:2301.07093, 2023.
- [29] Zhengqi Li and Noah Snavely. Megadepth: Learning single-view depth prediction from internet photos. In *Proceedings of the IEEE conference on computer vision and pattern recognition*, pages 2041–2050, 2018.
- [30] Ning Liao, Bowen Shi, Min Cao, Xiaopeng Zhang, Qi Tian, and Junchi Yan. Rethinking visual prompt learning as masked visual token modeling. *arXiv preprint arXiv:2303.04998*, 2023.
- [31] Chen-Hsuan Lin, Jun Gao, Luming Tang, Towaki Takikawa, Xiaohui Zeng, Xun Huang, Karsten Kreis, Sanja Fidler, Ming-Yu Liu, and Tsung-Yi Lin. Magic3d: High-resolution text-to-3d content creation. *arXiv preprint arXiv:2211.10440*, 2022.

- [32] Pengfei Liu, Weizhe Yuan, Jinlan Fu, Zhengbao Jiang, Hiroaki Hayashi, and Graham Neubig. Pre-train, prompt, and predict: A systematic survey of prompting methods in natural language processing. *ACM Computing Surveys*, 55(9):1–35, 2023.
- [33] Ruoshi Liu, Rundi Wu, Basile Van Hoorick, Pavel Tokmakov, Sergey Zakharov, and Carl Vondrick. Zero-1-to-3: Zero-shot one image to 3d object. arXiv preprint arXiv:2303.11328, 2023.
- [34] Xiao Liu, Kaixuan Ji, Yicheng Fu, Weng Lam Tam, Zhengxiao Du, Zhilin Yang, and Jie Tang. P-tuning v2: Prompt tuning can be comparable to fine-tuning universally across scales and tasks. *arXiv preprint arXiv:2110.07602*, 2021.
- [35] Xiao Liu, Yanan Zheng, Zhengxiao Du, Ming Ding, Yujie Qian, Zhilin Yang, and Jie Tang. Gpt understands, too. *arXiv preprint arXiv:2103.10385*, 2021.
- [36] Liying Lu, Wenbo Li, Xin Tao, Jiangbo Lu, and Jiaya Jia. Masa-sr: Matching acceleration and spatial adaptation for reference-based image super-resolution. In *Proceedings of the IEEE/CVF* Conference on Computer Vision and Pattern Recognition, pages 6368–6377, 2021.
- [37] Yiyang Ma, Huan Yang, Wenjing Wang, Jianlong Fu, and Jiaying Liu. Unified multi-modal latent diffusion for joint subject and text conditional image generation. *arXiv* preprint arXiv:2303.09319, 2023.
- [38] Ron Mokady, Amir Hertz, Kfir Aberman, Yael Pritch, and Daniel Cohen-Or. Null-text inversion for editing real images using guided diffusion models. arXiv preprint arXiv:2211.09794, 2022.
- [39] Chong Mou, Xintao Wang, Liangbin Xie, Jian Zhang, Zhongang Qi, Ying Shan, and Xiaohu Qie. T2i-adapter: Learning adapters to dig out more controllable ability for text-to-image diffusion models. *arXiv preprint arXiv:2302.08453*, 2023.
- [40] Alex Nichol, Prafulla Dhariwal, Aditya Ramesh, Pranav Shyam, Pamela Mishkin, Bob McGrew, Ilya Sutskever, and Mark Chen. Glide: Towards photorealistic image generation and editing with text-guided diffusion models. *arXiv preprint arXiv:2112.10741*, 2021.
- [41] Seoung Wug Oh, Sungho Lee, Joon-Young Lee, and Seon Joo Kim. Onion-peel networks for deep video completion. In *proceedings of the IEEE/cvf international conference on computer vision*, pages 4403–4412, 2019.
- [42] Ben Poole, Ajay Jain, Jonathan T Barron, and Ben Mildenhall. Dreamfusion: Text-to-3d using 2d diffusion. *arXiv preprint arXiv:2209.14988*, 2022.
- [43] Xuebin Qin, Zichen Zhang, Chenyang Huang, Masood Dehghan, Osmar R Zaiane, and Martin Jagersand. U2-net: Going deeper with nested u-structure for salient object detection. *Pattern recognition*, 106:107404, 2020.
- [44] Alec Radford, Jong Wook Kim, Chris Hallacy, Aditya Ramesh, Gabriel Goh, Sandhini Agarwal, Girish Sastry, Amanda Askell, Pamela Mishkin, Jack Clark, et al. Learning transferable visual models from natural language supervision. In *International conference on machine learning*, pages 8748–8763. PMLR, 2021.
- [45] Colin Raffel, Noam Shazeer, Adam Roberts, Katherine Lee, Sharan Narang, Michael Matena, Yanqi Zhou, Wei Li, and Peter J Liu. Exploring the limits of transfer learning with a unified text-to-text transformer. *The Journal of Machine Learning Research*, 21(1):5485–5551, 2020.
- [46] Aditya Ramesh, Prafulla Dhariwal, Alex Nichol, Casey Chu, and Mark Chen. Hierarchical text-conditional image generation with clip latents. *arXiv preprint arXiv:2204.06125*, 2022.
- [47] Aditya Ramesh, Mikhail Pavlov, Gabriel Goh, Scott Gray, Chelsea Voss, Alec Radford, Mark Chen, and Ilya Sutskever. Zero-shot text-to-image generation. In *International Conference on Machine Learning*, pages 8821–8831. PMLR, 2021.
- [48] Robin Rombach, Andreas Blattmann, Dominik Lorenz, Patrick Esser, and Björn Ommer. High-resolution image synthesis with latent diffusion models. In *Proceedings of the IEEE/CVF Conference on Computer Vision and Pattern Recognition*, pages 10684–10695, 2022.

- [49] Nataniel Ruiz, Yuanzhen Li, Varun Jampani, Yael Pritch, Michael Rubinstein, and Kfir Aberman. Dreambooth: Fine tuning text-to-image diffusion models for subject-driven generation. *arXiv* preprint arXiv:2208.12242, 2022.
- [50] Chitwan Saharia, William Chan, Saurabh Saxena, Lala Li, Jay Whang, Emily L Denton, Kamyar Ghasemipour, Raphael Gontijo Lopes, Burcu Karagol Ayan, Tim Salimans, et al. Photorealistic text-to-image diffusion models with deep language understanding. Advances in Neural Information Processing Systems, 35:36479–36494, 2022.
- [51] Thomas Schops, Johannes L Schonberger, Silvano Galliani, Torsten Sattler, Konrad Schindler, Marc Pollefeys, and Andreas Geiger. A multi-view stereo benchmark with high-resolution images and multi-camera videos. In *Proceedings of the IEEE Conference on Computer Vision* and Pattern Recognition, pages 3260–3269, 2017.
- [52] Jascha Sohl-Dickstein, Eric Weiss, Niru Maheswaranathan, and Surya Ganguli. Deep unsupervised learning using nonequilibrium thermodynamics. In *International Conference on Machine Learning*, pages 2256–2265. PMLR, 2015.
- [53] Kihyuk Sohn, Yuan Hao, José Lezama, Luisa Polania, Huiwen Chang, Han Zhang, Irfan Essa, and Lu Jiang. Visual prompt tuning for generative transfer learning. *arXiv* preprint *arXiv*:2210.00990, 2022.
- [54] Jiaming Song, Chenlin Meng, and Stefano Ermon. Denoising diffusion implicit models. arXiv preprint arXiv:2010.02502, 2020.
- [55] Roman Suvorov, Elizaveta Logacheva, Anton Mashikhin, Anastasia Remizova, Arsenii Ashukha, Aleksei Silvestrov, Naejin Kong, Harshith Goka, Kiwoong Park, and Victor Lempitsky. Resolution-robust large mask inpainting with fourier convolutions. In *Proceedings of the IEEE/CVF winter conference on applications of computer vision*, pages 2149–2159, 2022.
- [56] Shitao Tang, Jiahui Zhang, Siyu Zhu, and Ping Tan. Quadtree attention for vision transformers. *arXiv preprint arXiv:2201.02767*, 2022.
- [57] Andrey Voynov, Kfir Aberman, and Daniel Cohen-Or. Sketch-guided text-to-image diffusion models. *arXiv preprint arXiv:2211.13752*, 2022.
- [58] Xinlong Wang, Wen Wang, Yue Cao, Chunhua Shen, and Tiejun Huang. Images speak in images: A generalist painter for in-context visual learning. arXiv preprint arXiv:2212.02499, 2022.
- [59] Chenfei Wu, Jian Liang, Lei Ji, Fan Yang, Yuejian Fang, Daxin Jiang, and Nan Duan. Nüwa: Visual synthesis pre-training for neural visual world creation. In *Computer Vision–ECCV 2022: 17th European Conference, Tel Aviv, Israel, October 23–27, 2022, Proceedings, Part XVI*, pages 720–736. Springer, 2022.
- [60] Binxin Yang, Shuyang Gu, Bo Zhang, Ting Zhang, Xuejin Chen, Xiaoyan Sun, Dong Chen, and Fang Wen. Paint by example: Exemplar-based image editing with diffusion models. *arXiv* preprint arXiv:2211.13227, 2022.
- [61] Yuan Yao, Ao Zhang, Zhengyan Zhang, Zhiyuan Liu, Tat-Seng Chua, and Maosong Sun. Cpt: Colorful prompt tuning for pre-trained vision-language models. arXiv preprint arXiv:2109.11797, 2021.
- [62] Jiahui Yu, Xin Li, Jing Yu Koh, Han Zhang, Ruoming Pang, James Qin, Alexander Ku, Yuanzhong Xu, Jason Baldridge, and Yonghui Wu. Vector-quantized image modeling with improved vqgan. *arXiv preprint arXiv:2110.04627*, 2021.
- [63] Jiahui Yu, Yuanzhong Xu, Jing Yu Koh, Thang Luong, Gunjan Baid, Zirui Wang, Vijay Vasudevan, Alexander Ku, Yinfei Yang, Burcu Karagol Ayan, et al. Scaling autoregressive models for content-rich text-to-image generation. arXiv preprint arXiv:2206.10789, 2022.
- [64] Yu Zeng, Zhe Lin, Jimei Yang, Jianming Zhang, Eli Shechtman, and Huchuan Lu. High-resolution image inpainting with iterative confidence feedback and guided upsampling. In *Computer Vision–ECCV 2020: 16th European Conference, Glasgow, UK, August 23–28, 2020, Proceedings, Part XIX 16*, pages 1–17. Springer, 2020.

- [65] Chenshuang Zhang, Chaoning Zhang, Mengchun Zhang, and In So Kweon. Text-to-image diffusion model in generative ai: A survey. *arXiv preprint arXiv:2303.07909*, 2023.
- [66] Lymin Zhang and Maneesh Agrawala. Adding conditional control to text-to-image diffusion models. *arXiv preprint arXiv:2302.05543*, 2023.
- [67] Yuanhan Zhang, Kaiyang Zhou, and Ziwei Liu. What makes good examples for visual in-context learning? *arXiv preprint arXiv:2301.13670*, 2023.
- [68] Liang Zhao, Xinyuan Zhao, Hailong Ma, Xinyu Zhang, and Long Zeng. 3dfill: Reference-guided image inpainting by self-supervised 3d image alignment. arXiv preprint arXiv:2211.04831, 2022.
- [69] Shengyu Zhao, Jonathan Cui, Yilun Sheng, Yue Dong, Xiao Liang, Eric I Chang, and Yan Xu. Large scale image completion via co-modulated generative adversarial networks. *arXiv* preprint *arXiv*:2103.10428, 2021.
- [70] Yunhan Zhao, Connelly Barnes, Yuqian Zhou, Eli Shechtman, Sohrab Amirghodsi, and Charless Fowlkes. Geofill: Reference-based image inpainting of scenes with complex geometry. *arXiv* preprint arXiv:2201.08131, 2022.
- [71] Bolei Zhou, Agata Lapedriza, Aditya Khosla, Aude Oliva, and Antonio Torralba. Places: A 10 million image database for scene recognition. *IEEE transactions on pattern analysis and machine intelligence*, 40(6):1452–1464, 2017.
- [72] Yuqian Zhou, Connelly Barnes, Eli Shechtman, and Sohrab Amirghodsi. Transfill: Reference-guided image inpainting by merging multiple color and spatial transformations. In *Proceedings of the IEEE/CVF conference on computer vision and pattern recognition*, pages 2266–2276, 2021.

#### A Broader Impacts

This paper exploited image manipulations and synthesis with text-to-image models. Because of their impressive generative abilities, these models may produce misinformation or fake images. So we sincerely remind users to pay attention to it. Besides, privacy and consent also become important considerations, as generative models are often trained on large-scale data. Furthermore, generative models may perpetuate biases present in the training data, leading to unfair outcomes. Therefore, we recommend users be responsible and inclusive while using these text-to-image generative models. Note that our method only focuses on technical aspects. Both images and pre-trained models used in this paper are all open-released.

## **B** Additional Results

In this section, we provide more experiment results and in-depth analyses about the attention and inference cost of the proposed Prompt-Guided In-Context Inpainting (PGIC).

# **B.1** Self-Attention Analysis

We show the visualization of self-attention scores attended by masked regions for reference-guided inpainting with different DDIM [54] steps in Fig. 8. For a more explicit expression, we mask out uninterested scores from unmasked regions and only display the attention map in the reference view as in Alg. 1. We select two representative attention layers with feature scales of 1/32 and 1/8, enabling us to observe both high-level and fine-grained attention aggregations. From Fig. 8, self-attention can successfully capture correct feature correlations without any backbone fine-tuning. As diffusion sampling progresses, self-attention modules gradually shift their focus from specific key points to broader related regions, which is convincing and intuitive. Because the key landmarks help to swiftly locate the spatial correlation between the reference and target, while the extended receptive fields further refine the generation for the following sampling steps.

#### **Algorithm 1** Pseudo codes for the attention visualization.

```
# x: [b,2hw,c], input feature for attention module (left:reference, right:target)
# mask: [b,2hw,1], input 0-1 mask; 1 means masked regions

q, k = matmul(x, Wq), matmul(x, Wk) # [b,2hw,c], project x to query (q) and key (k)
A = matmul(q, k.T) # [b,2hw,2hw], get attenion map
A = mean(A * mask , dim=1) # [b,2hw] get mean scores attended by masked regions
A = A.reshape(b,h,w)[:, :, :w//2] # [b,h,w], show reference attention score only
```

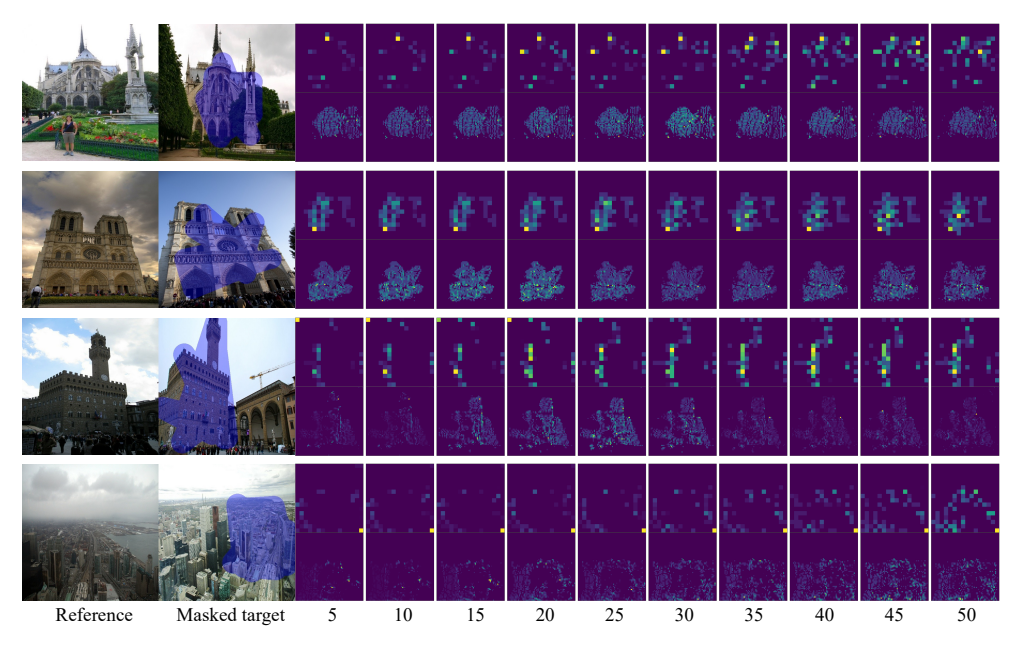


Figure 8: The visualization of attention scores in PGIC for reference-guided inpainting with different DDIM steps. We show the scores from reference views that are attended by masked regions. The upper row shows attention scores from the 8th/16 self-attention layer (1/32 scale), while the bottom row shows ones from the 14th/16 self-attention layer (1/8 scale).

#### **B.2** Reference-Guided Inpainting on Real-World Data

We compare PGIC with TransFill [72] on the officially provided real-world dataset in Tab. 9 and Fig. 10. Since most instances are defined as object removal tasks without ground truth, quantitative metrics are for reference only. PGIC still outperforms TransFill and ProFill [64] in FID and LPIPS with perceptually pleasant results. Moreover, as shown in Fig. 10, PGIC enjoys good generalization in unseen or occluded regions, because it gets rid of the constrained geometric warping.

#### **B.3** Inference Speed

We provide the inference speed for different input resolutions in Tab. 7. All tests are based on one 32GB V100 GPU with 50 DDIM steps. PGIC needs to stitch two images together, which would double the input size. But the inference time is not doubled as shown in Tab. 7. Note that when the image size is smaller than 512, the difference in inference costs is not obvious. Therefore, we think that the inference cost of the proposed PGIC is still acceptable in most real-world applications.

Table 7: Inference speed of SD [48] under 50 DDIM sampling steps.

Input	sec/img
256×256 256×512 512×512 512×1024	2.9172 2.9395 3.0715 4.0205
256×512 512×512	2.9395 3.0715

#### **B.4** More Qualitative and Quantitative Results

**Qualitative Results.** We show more qualitative results for image inpainting (Fig. 11), outpainting (Fig. 12), reference-guided inpainting (Fig. 13), local SR (Fig. 14), and novel view synthesis (Fig. 15).

**Quantitative Comparison on Local SR.** More quantitative results on local SR compared with Tab. 10. Although SR-specific LIIF [8] and reference-based MASA-SR [36] achieve better metrics,

the performance limitation of PGIC may suffer from the highly compressed latent inputs (1/8) as mentioned in the limitation of [48] and without training with perceptual loss [25]. Note PGIC enjoys competitive or superior qualitative results compared with LIIF [8] and MASA-SR [36] as in Fig. 14.

**Diversity of Novel View Synthesis.** Besides, we show some diverse novel view syntheses on Objaverse [12] in Fig. 16. Different random seeds are utilized to process the DDIM sampling. PGIC can achieve reasonable results with correct target poses.

**Inpainting with Unrelated Reference.** We provide some interesting explorations about using unrelated references searched on the Internet to guide the image inpainting in Fig. 17. Our PGIC enjoys a certain generalization to produce perceptually reasonable results even with unrelated references.

## C Implementation and Training Details

#### **C.1** Prompt Initialization

As discussed in the ablation study of the main paper, we initialize all prompt embeddings with the mean feature of task-specific descriptions. In this section, we introduce these descriptions in detail.

**Inpainting&Outpainting.** The description is "Inpaint the given image with visually coherent and high-fidelity background and texture".

**Reference-Guided Inpainting.** The description is "The whole image is split into two parts with the same size, they share the same scene/landmark captured with different viewpoints and times".

**Local SR.** The description is "The right image is the magnified high-resolution patch of the left image's red square".

**Novel View Synthesis.** The description is "Left is the reference image, while the right one is the target image with a different viewpoint. The relative pose:". Note that our encoded pose embedding is concatenated to the end of the task description embeddings.

## C.2 Datasets and Data Formulation

Image Inpainting & Outpainting. The inpainting is evaluated on Places2 [71] in  $512 \times 512$ . We only prompt-tuned on the 250k Places2 subset with random masking from [13]. 1,000 images are used as the validation for inpainting. The outpainting is evaluated on Flickr-Scenery [9] with an official training/testing split. For the outpaint training, we randomly mask 25% to 75% for each image. While the testing is based on a 50% masking rate to extend both sides from  $512 \times 512$  to  $512 \times 2048$ .

**Reference-guided Inpainting.** As mentioned in the main paper, we retain image pairs from MegaDepth [29] with 40% to 70% co-occurrence with about 80k images and 820k pairs in  $512 \times 512$ . We split 505 pairs as the validation, including some manual masks from ETH3D scenes [51]. For the matching-based mask used for reference-guided inpainting, we first filter matching results from [56] with a threshold of 0.8. Then we randomly crop the matching bounding box into a 20% to 50% sub-space. Finally, 15 to 30 vertices in the cropped bounding box are sampled for mask generation.

**Local Super-Resolution.** We evaluate the local SR on the mixed DIV2K and Flickr2K [1] in  $256 \times 256$ . Our test set contains 200 images from both DIV2K and Flickr2K, while 3 patches are chosen from each reference image. Thus there are 600 test samples in all. During the training, we randomly frame low-resolution patches from  $48 \times 48$  to  $72 \times 72$ , while testing is based on 64 to 256.

Novel View Synthesis. For the novel view synthesis on Objaverse [12], Zero123 [33] provided images including 800k various scenes with object masks. For each scene, 12 images are rendered in  $256\times256$  with different viewpoints. We select 500 scenes as the validation, while others are used as the training set. Following [33], the spherical coordinate system is used to convert the relative pose  $\Delta p$  into the polar angle  $\theta$ , azimuth angle phi, and radius r distanced from the canonical center as  $\Delta p = (\Delta \theta, \sin\Delta \phi, \cos\Delta \phi, \Delta r)$ , where the azimuth angle is sinusoidally encoded to address the non-continuity. For the masking of Objaverse images, we dilate the object mask and related bounding box with 10 to 25 kernel size and 5% to 20% respectively. Then we randomly sample 20 to 45 points to paint the irregular masks.

Table 8: Training details of PGIC.	'Ref. inpainting'	means reference-guided inpainting, while 'NVS'
means novel view synthesis.		

Task	Batch size	Learning Prompt&LoRA		Steps	Training time
Inpainting	32	3e-5	/	8.5k	6h
Outpainting	32	3e-5	/	8.5k	6h
Ref. inpainting	16	3e-5	/	6k	11h
Local SR	32	1e-4	/	15k	15h
NVS	48	1e-4	1e-5	80k	34h

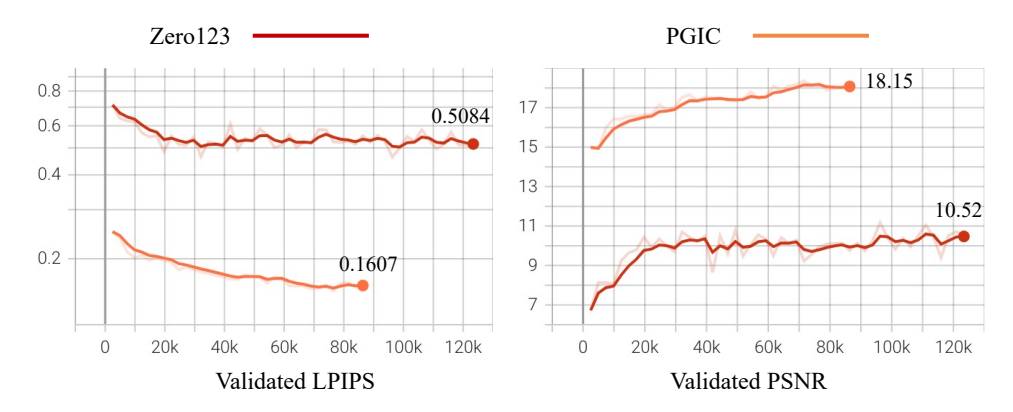


Figure 9: Training processes of PGIC and Zero123 [33] of the novel view synthesis on Objaverse [12].

#### **C.3** Training Details

We first show the training details in Tab. 8. It shows that PGIC is efficient to be trained for various tasks. To further demonstrate the effectiveness of PGIC, we provide the training log of PGIC and Zero123 in Fig. 9. Obviously, the in-context inpainting-based PGIC enjoys a substantially faster convergence and superior performance.

#### **D** Limitation and Future Works

Although PGIC enjoys good performance in reference-guided inpainting, without the dependence on 3D geometric warping, it may suffer from a little geometric error. For example, PGIC could not align the proportions among different buildings properly. Since the generated results are perceptually good, such geometric error is hard to be recognized. Besides, PGIC randomly produces plausible appearances in unseen regions during the novel view synthesis, which may break the consistency during the long sequence generation. So maintaining the long sequence consistency is future work.

# **E** Preliminary

**Diffusion Models (DMs)** [52] adopt Markov Chain of length *T* to connect the real data distribution and the random Gaussian distribution. The forward process gradually adds Gaussian noise to the real image, while the reverse process gradually denoises the image. DMs are trained to estimate the noise added to the image [19]. Moreover, the DDIM [54] sampler is widely used to speed up the denoising process with fewer steps.

Latent Diffusion Model (LDM) [48] compresses inputs x into latent features z with much lower spatial scales to reduce the computation cost of the diffusion model. LDM further fine-tunes the diffusion model for the text-guided inpainting task such that the diffusion model can focus on generating masked regions based on unmasked ones and text prompts. In this task, the objective is

$$\mathcal{L}_{LDM} = \mathbb{E}_{x,\epsilon \sim \mathcal{N}(0,\mathcal{I}),t} \left[ \|\varepsilon - \varepsilon_{\theta} \left( [z_t; \hat{z}_0; \mathbf{M}], t \right) \|^2 \right], \tag{2}$$

Table 9: Reference-guided inpainting results on the real-world set provided by TransFill [72].

Method	PSNR↑	SSIM↑	FID↓	LPIPS↓
ProFill [64]	25.550	0.944	71.758	0.0848
TransFill [72]	<b>26.052</b>	<b>0.945</b>	62.493	0.0757
PGIC	25.733	0.942	<b>61.276</b>	<b>0.0756</b>

Table 10: Results for local SR on mixed DIV2K/Flickr2K testset compared with SR methods [8; 36].

Methods	PSNR↑	SSIM↑	FID↓	LPIPS↓
LIIF [8]	<b>29.518</b> 25.872 24.379 25.589	0.889	37.331	0.2227
MASA-SR [36]		0.807	<b>36.074</b>	<b>0.1296</b>
LDM (SR)		0.790	46.716	0.2005
PGIC		0.798	38.477	0.1556

where  $\varepsilon_{\theta}(\cdot)$  is the estimated noise by LDM,  $z_t$  is a noisy latent feature of input  $z_0$  in step t;  $\hat{z}_0 = z_0 \odot (1 - \mathbf{M})$  are masked latent features that are concatenated to  $z_t$  with mask  $\mathbf{M}$ . During the inpainting training, masked and unmasked regions are learned with inherent self-attention modules in pre-trained LDM, which lays the foundation of the PGIC.

**Text-to-Image Models.** Recent pioneering achievements on T2I could be generally categorized into AutoRegressive (AR) [14; 47; 63]/Non-AutoRegressive (NAR) [7], and Diffusion Models (DMs) [40; 46; 50; 48]. All T2I methods learn text features through pre-trained text encoders (e.g., CLIP [44]). For the vision branch, AR/NAR models usually depend on quantized image modeling [14; 62] to downsample image features spatially. Then, transformer-based models are focused on predicting visual sequences according to text prompts. On the other hand, DMs [19] have come into prominence recently, with impressive generated results. GLIDE [40] first used DM to address T2I enhanced with Classifier-Free Guidance (CFG) [20]. Imagen [50] found that larger Language Models (LMs) [45] benefit T2I a lot. LDM [48] inherited the advantage of quantized image modeling, which effectively saved computations. We find that all these T2I models share the same commonality, i.e., they have self and cross-attention modules for learning correlations between image-to-image and text-to-image. Theoretically, all these T2I models can be strengthened by our PGIC. We choose SD as the baseline because it is one of the most powerful open-released T2I models.

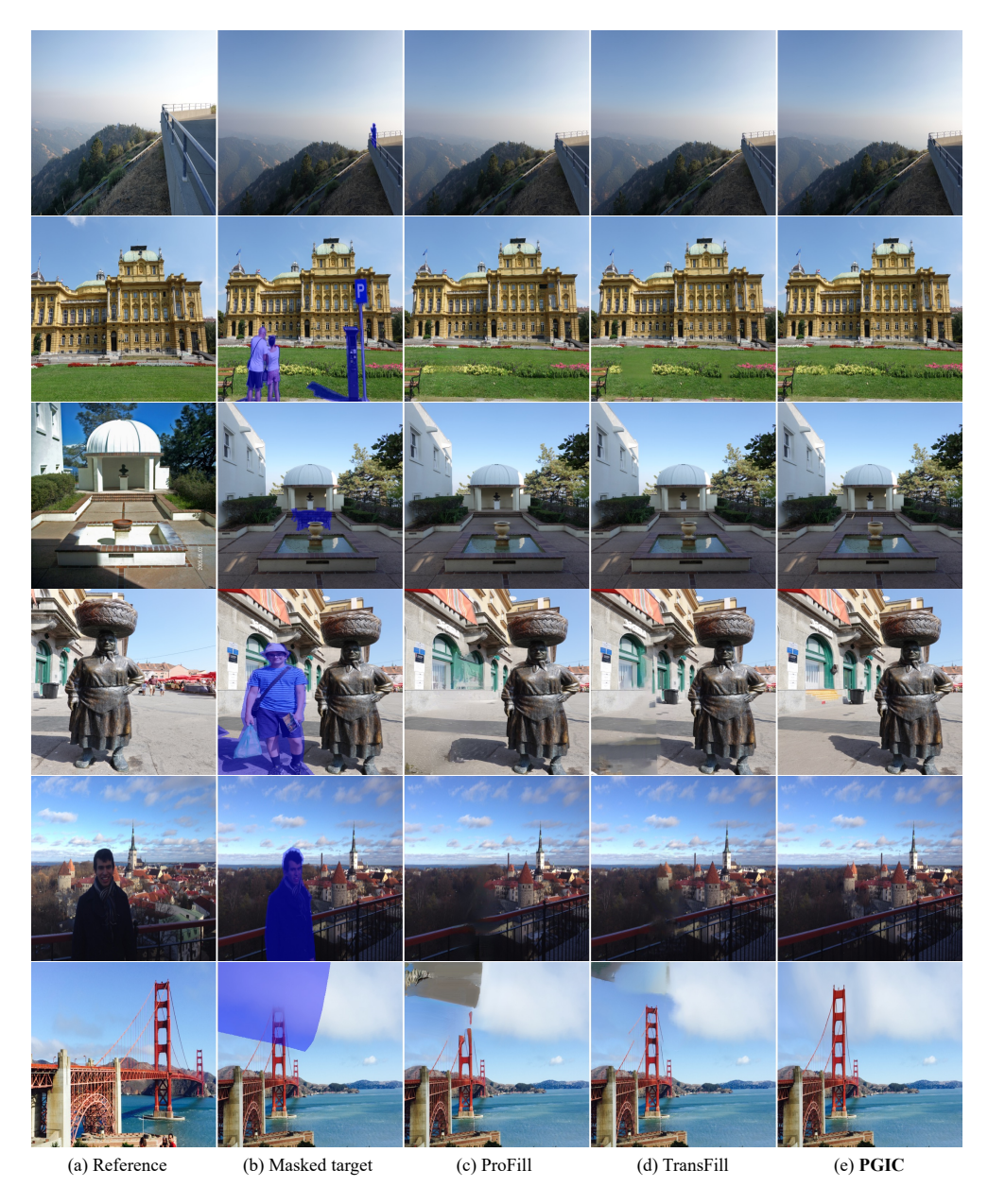


Figure 10: Qualitative reference-guided inpainting results compared with ProFill [64], TransFill [72], and our PGIC on the challenging real set provided by TransFill [72].

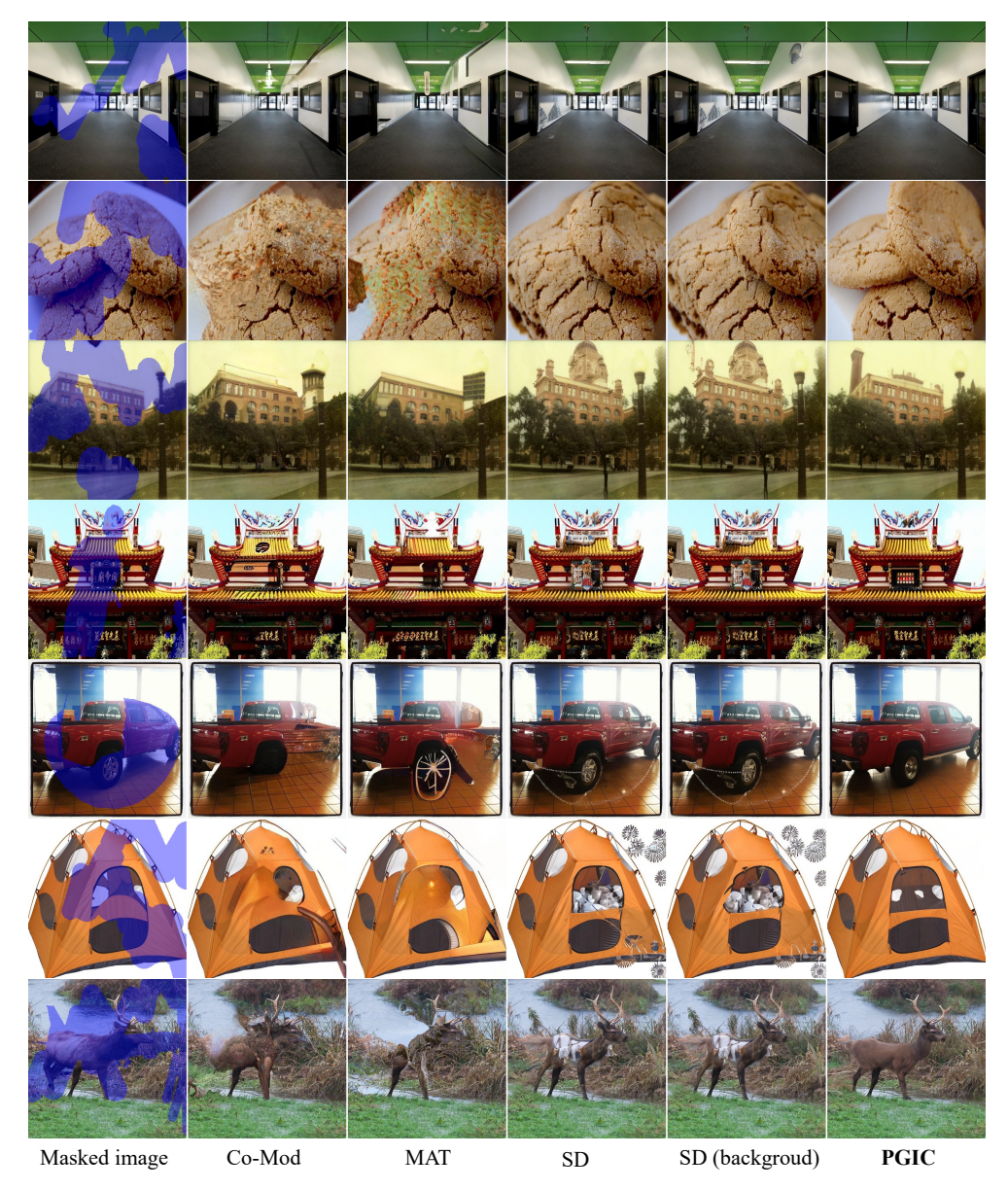


Figure 11: Inpainting results compared with Co-Mod [69], MAT [27], SD [48] and our PGIC on Places2 [71].

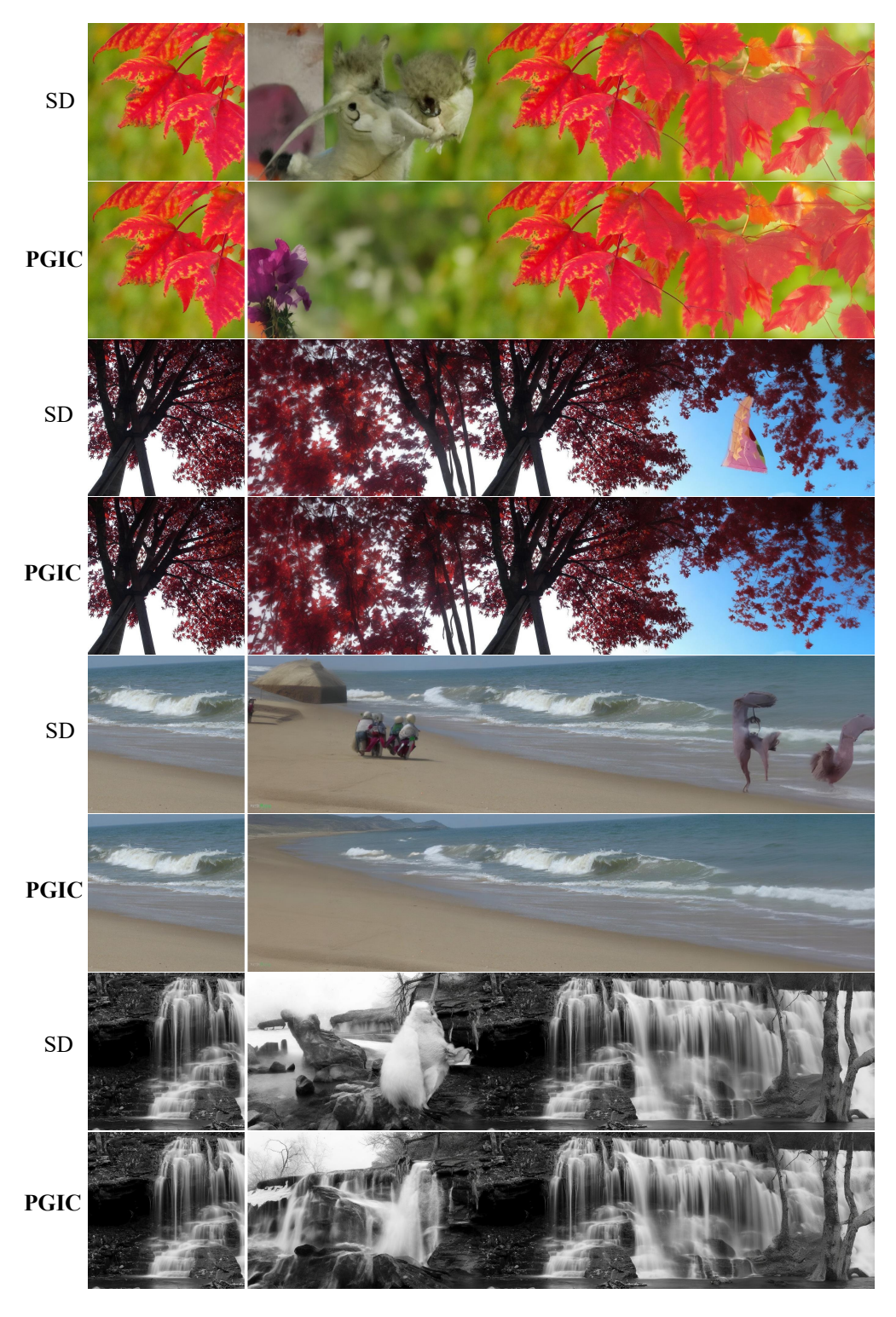


Figure 12: Outpainting results compared with SD [48] and our PGIC on Flickr-Scenery [9].



Figure 13: Qualitative reference-guided inpainting results on MegaDepth, which are compared among (c) SD [48], (d) ControlNet [66]+Matching [56], (e) Perceiver [23] with ImageCLIP [44], (f) Paint-by-Example [60], (g) TransFill [72], and (I) our PGIC. Please zoom in for more details.



Figure 14: Qualitative local SR results. (c) bicubic, (d) LIIF [8], (e) MASA-SR [36], (f) LDM (SR) [48], (g) PGIC (prompt tuning), and (h) PGIC based on LoRA on DIV2K and Flickr2K.

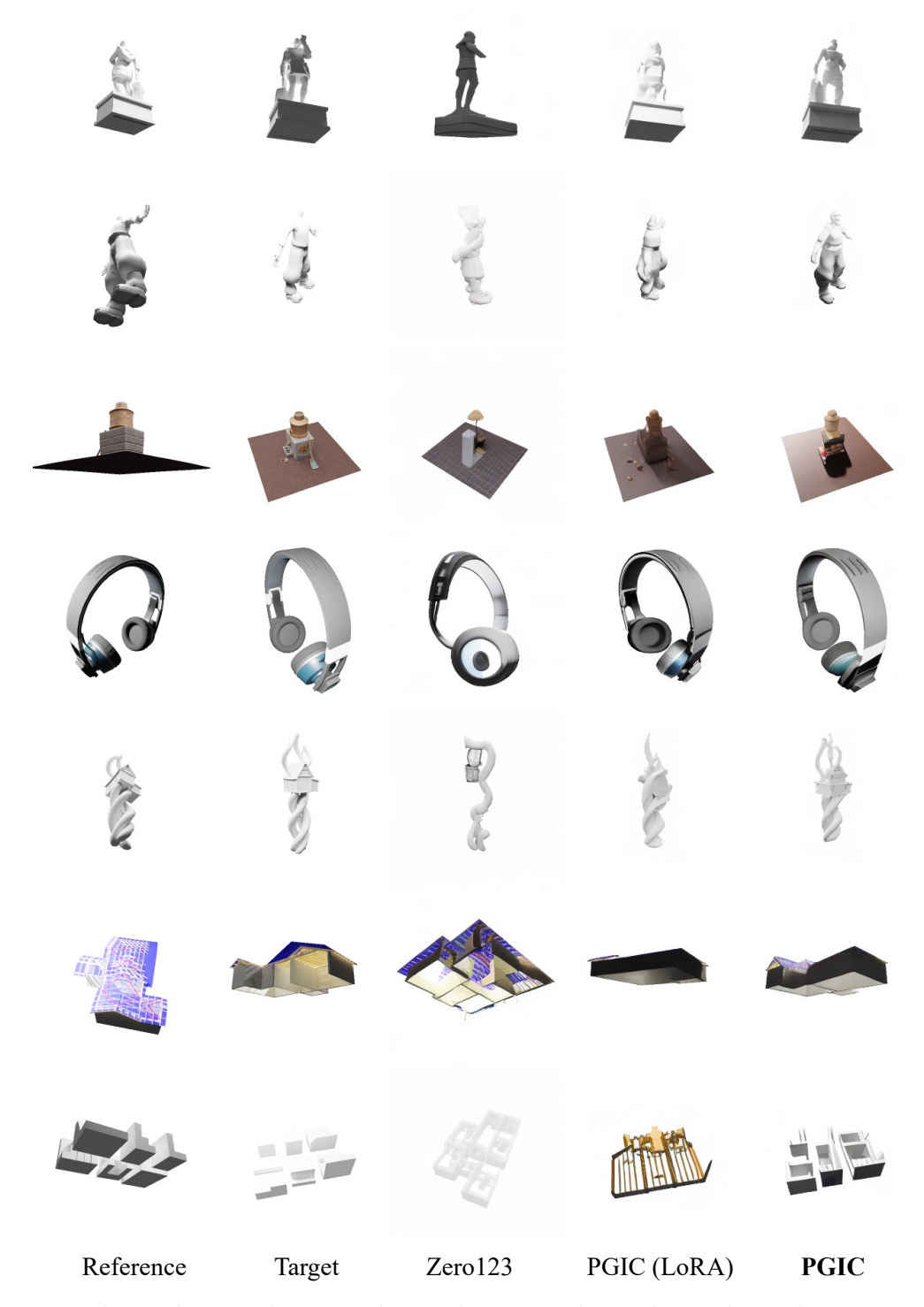


Figure 15: Novel view synthesis on Objaverse [12] from a single reference image.

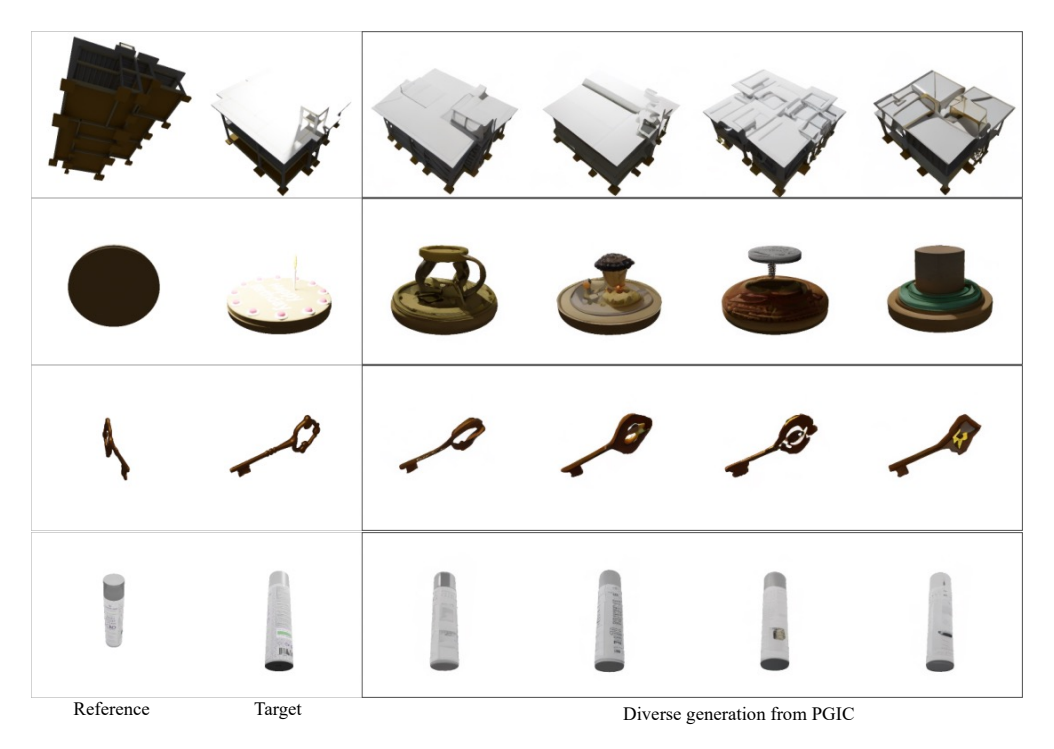


Figure 16: Diversity of the novel view synthesis on Objaverse [12] from a single reference image.

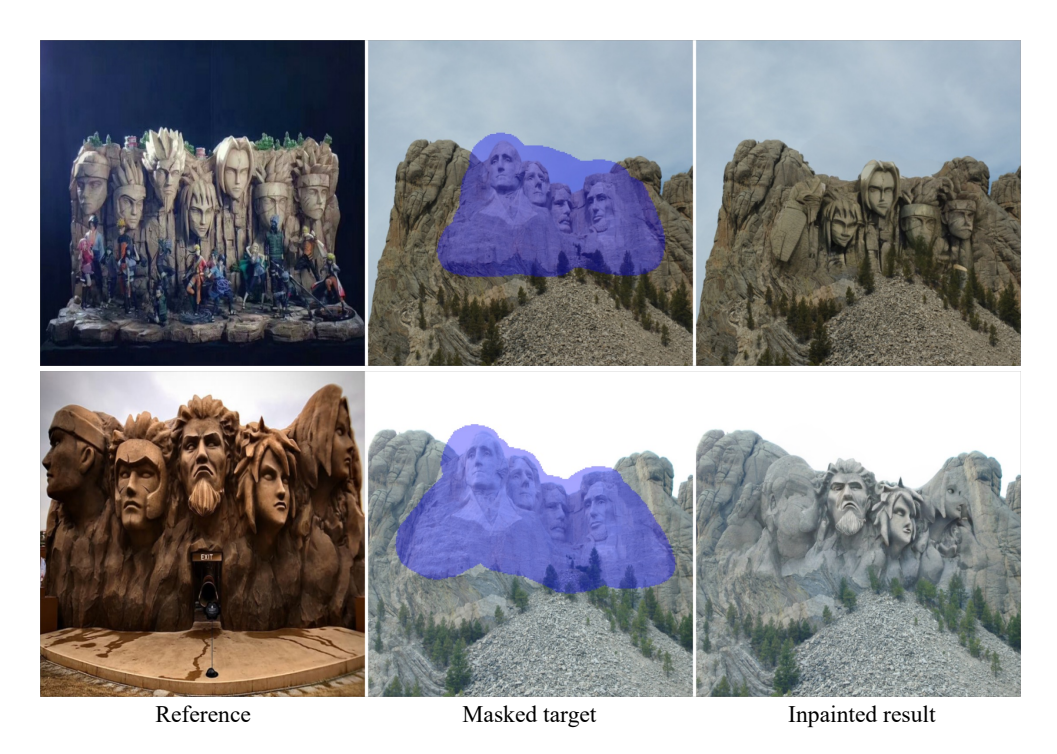


Figure 17: Unrelated reference-guided inpainting addressed by PGIC.